

## Joint Cosmic Microwave Background and Weak Lensing Analysis: Constraints on Cosmological Parameters

Carlo R. Contaldi,<sup>\*</sup> Henk Hoekstra,<sup>†</sup> and Antony Lewis

*CITA, University of Toronto, 60 St. George Street, Toronto, M5S 3H8, Ontario, Canada*

(Received 24 February 2003; published 6 June 2003)

We use cosmic microwave background (CMB) observations together with the red-sequence cluster survey weak lensing results to derive constraints on a range of cosmological parameters. This particular choice of observations is motivated by their robust physical interpretation and complementarity. Our combined analysis, including a weak nucleosynthesis constraint, yields accurate determinations of a number of parameters including the amplitude of fluctuations  $\sigma_8 = 0.89 \pm 0.05$  and matter density  $\Omega_m = 0.30 \pm 0.03$ . We also find a value for the Hubble parameter of  $H_0 = 70 \pm 3 \text{ km s}^{-1} \text{ Mpc}^{-1}$ , in good agreement with the Hubble Space Telescope key-project result. We conclude that the combination of CMB and weak lensing data provides some of the most powerful constraints available in cosmology today.

DOI: 10.1103/PhysRevLett.90.221303

PACS numbers: 98.80.Es, 98.62.Sb, 98.70.Vc

The physics behind the anisotropies we see in the microwave background is well studied and understood. The evolution of the photon distribution function in the tight coupling era and through decoupling is well inside the linear perturbation regime and is the reason for the cosmic microwave background's (CMB) unique status as a probe of cosmological models. The *physical* interpretation of the angular power spectrum of primary CMB anisotropies is unambiguous when restricted to the inflationary paradigm and given a suitably parametrized spectrum of initial perturbations.

The recently released Wilkinson Microwave Anisotropy Probe (WMAP) first year results [1] have revealed the CMB angular power spectrum with unprecedented accuracy to multipoles below  $\ell = 900$  [2]. The results are a stunning confirmation of the acoustic oscillation picture, with perturbations arising from an initial superhorizon spectrum of predominantly adiabatic fluctuations, as predicted, for example, by simple inflationary models. The measurements of the first two acoustic peaks has confirmed in precise detail earlier detections of the peak/dip pattern on scales below the sound horizon at last scattering [3–9].

On its own, the current picture of the CMB made up of the WMAP results together with high resolution cosmic background imager (CBI) and arcminute cosmology bolometer array receiver (ACBAR) (WMAPext combination) observations implies tight constraints on a number of parameters [10,11]; the curvature in units of critical density  $\Omega_K$  and various other parameters in the combinations determined by the physical mechanisms which give rise to the observed CMB anisotropy. In addition, the measurement of a cross correlation between the polarization and temperature anisotropy [12,13] is the first significant detection of reionization in the CMB, which gives a constraint on the optical depth to the last scattering surface.

Although the CMB data alone provide tight constraints on some parameter combinations, other combinations are very poorly constrained due to partial degeneracies. The addition of other data such as measurements of the matter power spectrum  $P(k)$  is essential to break these degeneracies and tightly constrain the parameters of most interest individually. One way to infer the matter power spectrum is to rely on visible tracers of the (dark) matter distribution such as galaxy redshift surveys or observations of the Lyman- $\alpha$  forest. The Lyman- $\alpha$  forest gives a way to measure the linear power spectrum of neutral gas at redshifts higher than those probed by galaxy surveys.

The combination of CMB, two degree field galaxy redshift survey (2dFGRS) [14], and Lyman- $\alpha$  forest data [15] yields tight constraints on the density of dark matter and vacuum energy, and also reveal an indication of a running of the scalar spectral index characterized by the parameter  $dn_s/d \ln k$  [10]. However, inferring the matter power spectrum using these techniques involves a heuristic treatment of the relation between the tracers and the dark matter usually referred to as “biasing” [16]. As we enter the much heralded era of precision observations, such heuristic treatments might limit the accuracy with which parameters can be determined. A direct measurement of the power spectrum would not suffer from such limitations.

In terms of physical interpretation, measurements of the lensing signal induced by the large scale structure (LSS) (cosmic shear) hold a unique position in the growing set of observational tools available to cosmologists; it is a *direct* probe of the projected matter power spectrum over a redshift range determined by the lensed sources and over scales ranging from the linear to nonlinear regime. The intervening LSS induces a small, coherent correlation in the shapes of the background galaxies which today can be measured accurately [17–20]. The use of weak lensing data is not without challenges: the

small signal requires large survey areas and a careful removal of the observational distortions. However, separation of the shear signal into gradient (“*E*-type”) and curl (“*B*-type”) components provides a control on systematics including the presence of intrinsic alignments of nearby galaxies or systematically induced distortions in the image. The red-sequence cluster survey (RCS) 53 sq deg results used in this work [21] have a low *B*-type component on large scales together with a well determined redshift distribution of background sources.

In this Letter we present results from cosmological parameter fits using only CMB and weak lensing data. The motivation for this approach is to provide constraints on parameters using only observables with robust physical interpretations.

To evaluate the posterior distribution of the parameters of interest from the data we use an extension of the publicly available Markov Chain Monte Carlo package COSMOMC [22], as described in [23]. We calculate the likelihood of each cosmological model with respect to a combination of CMB and RCS data. The CMB data consists of WMAP data below  $\ell = 900$  and CBI, ACBAR, and very small array band powers above  $\ell = 800$  where the WMAP data is noise dominated and hence the band powers are essentially independent. To compare each angular power spectrum to the WMAP data we use the likelihood calculation routine made available by the WMAP team [11].

For each model we also calculate the mass aperture variance  $\langle M_{ap}^2(\theta) \rangle$  [24] at each aperture  $\theta$  sampled by the RCS results [21]. The mass aperture variance is a narrow filter of the convergence power spectrum  $P_\kappa(\ell)$  defined as

$$P_\kappa(\ell) = \frac{9}{4} \left( \frac{H_0}{c} \right)^4 \Omega_m^2 \int_0^{\chi_H} d\chi \frac{g^2(\chi)}{a^2(\chi)} P_{3D} \left( \frac{\ell}{f_K(\chi)}; \chi \right), \quad (1)$$

where  $\chi$  is the radial coordinate and  $f_K(\chi)$  is the comoving angular diameter distance to  $\chi$ .  $P_{3D}(k, \chi(z))$  is the 3D power spectrum of matter fluctuations. For each model we use the matter power spectrum calculated by CAMB [25] at  $z = 0$  and rescale to  $z > 0$  using the solution for growth of linear perturbations. To include the nonlinear contribution to the power spectrum at each redshift we use the HALOFIT procedure [26]. The procedure has been calibrated using numerical simulations of structure formation and is significantly more accurate than the previous procedure by Peacock and Dodds [27]. In particular it reproduces accurately, with rms errors of a few percent, the full nonlinear spectrum in standard  $\Lambda$ CDM (cold dark matter models with a cosmological constant) down to scales  $k \sim 10h \text{ Mpc}^{-1}$ . The accuracy of the HALOFIT procedure is adequate for current weak lensing data although future surveys will require more accurate estimates of the full, nonlinear power spectrum. This will most probably require the use of large numbers of numerical simulations to calibrate directly the nonlinear evolution in the full parameter space.

The function  $g(\chi) = \int_{\chi'}^{\chi_H} d\chi' p(\chi') f_K(\chi' - \chi) / f_K(\chi')$  is the source-averaged distance ratio where  $p(\chi(z))$  describes the redshift distribution of sources in the shear survey which is approximated by the function  $p(z) \sim (z/z_s)^\alpha \exp[-(z/z_s)^\beta]$ . The values  $\alpha = 4.7$ ,  $\beta = 1.7$ , and  $z_s = 0.302$  give the best fit to the observed redshift distribution. To allow for the uncertainty in the mean redshift of the distribution we marginalize over the range of values  $z_s \in [0.274, 0.337]$  for each likelihood evaluation. This corresponds to the  $\pm 3\sigma$  range indicated by the  $\chi^2$  of the fit to the photometric redshift distribution. The mean redshift for this choice of parameters is  $\langle z \rangle = 0.54\text{--}0.66$ . We assume a Gaussian prior for  $z_s$  in this range.

For each model sampled by the Monte Carlo chain we calculate the log likelihood with respect to the RCS data,

$$\ln L = -\frac{1}{2} (\langle \tilde{M}_{ap}^2 \rangle_i - \langle M_{ap}^2 \rangle_i) C_{ij}^{-1} (\langle \tilde{M}_{ap}^2 \rangle_j - \langle M_{ap}^2 \rangle_j), \quad (2)$$

where  $\langle \tilde{M}_{ap}^2 \rangle_i$  is the observed mass aperture variance at an aperture  $\theta_i$  and  $C_{ij}$  is the covariance matrix of the data [21]. This result is added to the log likelihoods from the CMB fit for the same model to obtain the full likelihood with respect to both CMB and RCS data.

We sample the probabilities with respect to six basic cosmological parameters: the physical densities of baryons  $\Omega_b h^2$ , and cold dark matter  $\Omega_c h^2$ , the Hubble parameter  $H_0 \equiv 100h \text{ km s}^{-1} \text{ Mpc}^{-1}$ , a reionization redshift parameter  $z_{\text{re}}$ , and a constant spectral index  $n_s$  and amplitude  $A_s$  of the initial scalar curvature perturbations. We assume the universe is spatially flat, with purely adiabatic perturbations evolving according to general relativity. The density of a cosmological constant-type component  $\Omega_\Lambda$  follows from  $\Omega_\Lambda = 1.0 - \Omega_m$ . We generated 16 converged Monte Carlo chains using the CMB data only, removed burn in and thinned to obtain fairly independent samples. The matter power spectrum and RCS likelihood was then computed for each sample, and importance sampling was used to adjust the chain weights accordingly (see [23]). The resultant set of weighted samples for the full posterior distribution from the CMB and RCS data were then used to compute our results. The only external prior assumed is a conservative big bang nucleosynthesis (BBN) Gaussian prior of the form  $\Omega_b h^2 = 0.022 \pm 0.002 (1\sigma)$  [28]. We include this prior to partially break the remaining  $n_s\text{--}\Omega_b h^2\text{--}\tau\text{--}A_s$  degeneracy in the CMB data. The action of this is similar to the  $\tau < 0.3$  prior adopted in the WMAP analysis [10,11].

From the set of samples it is simple to also compute the posterior distribution of other derivable quantities such as the rms amplitude of matter fluctuations on  $8h^{-1} \text{ Mpc}$  scales assuming linear evolution  $\sigma_8$ , the total matter density  $\Omega_m$ , the optical depth to last scattering  $\tau$ , and the age of the universe. In this Letter we do not consider tensor perturbations, dynamical dark energy candidates, or a running spectral index. We will explore

the constraints on these generalized models from CMB and weak lensing data future work.

The set of samples from the full six-dimensional parameter space can be used to evaluate marginalized parameter distributions by evaluating the weighted number density of samples ignoring the values of the parameters marginalized over. In Fig. 1 we show the one-dimensional marginalized distributions for a number of parameters. Each panel compares the distribution obtained using CMB data with that obtained using CMB and RCS data together; both also include the weak BBN prior discussed above. The effect of adding the weak lensing results is clearly seen in a number of parameters.

In Table I we summarize the marginalized constraints for a number of fundamental and derived parameters. We show the results obtained with and without inclusion of the RCS data. The addition of RCS data reduces the errors on  $\sigma_8$ ,  $\Omega_m$ ,  $H_0$ ,  $\Omega_\Lambda$ , and  $\Omega_c h^2$ . We also show constraints on the “classical” combinations probed by LSS data, namely, the constrained direction  $\sigma_8 \Omega_m^{0.5}$  and the shape parameter  $\Gamma \approx \Omega_m h$ .

It is instructive to look at the marginalized, two-dimensional likelihood in the  $(\Omega_m, \sigma_8)$  plane to understand how drastic improvements in the determination of the two parameters are obtained (Fig. 2). The RCS data alone is near degenerate in a particular direction while CMB data alone provides broad constraints in a quasi-orthogonal direction to RCS. The combination of the two data sets gives a much tighter confidence region. The

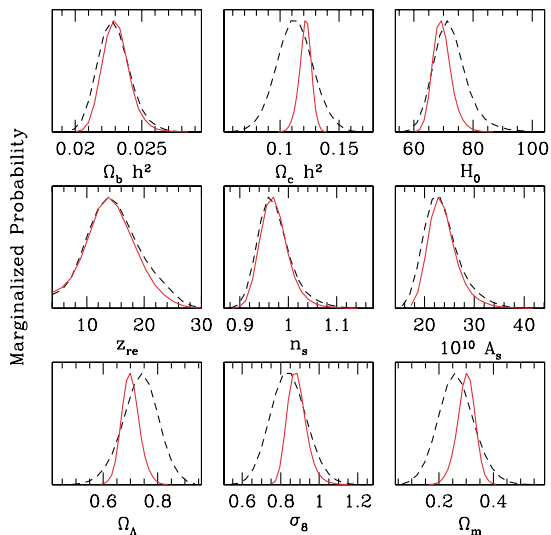


FIG. 1 (color online). One-dimensional, marginalized probability distributions for a selection of parameters. The dashed curves are for CMB only. The solid curves include the RCS data. We see the weak lensing data, while being consistent with the CMB only results, narrow down a number of distributions considerably. In particular, the combination of data provides a tight independent constraint on  $H_0$ . The matter density and fluctuation amplitude are also much better constrained with the combination of CMB and weak lensing than with just CMB.

region of intersection in six dimensions has slightly above average CMB likelihood, as is readily assessed using the importance weighted samples, so the data sets are highly consistent even in the full parameter space. The spread of the CMB posterior in the direction of the RCS degeneracy is largely due to the uncertainty remaining in the optical depth, as is clear for the tight constraint for  $\sigma_8 e^{-\tau}$  given in Table I.

Overall, our results are consistent with similar constraints from a combination of CMB, 2dFGRS, and Lyman- $\alpha$  data [1,10] with similar or smaller errors. The values obtained for  $\sigma_8$  using the WMAP data are somewhat higher than those obtained previously from CMB data due to the new evidence for a significant optical depth and a slightly higher anisotropy amplitude than previous observations indicated [2]. This is still lower, although not inconsistent, with estimates of  $\sigma_8$  from a possible Sunyaev-Zeldovich effect (SZE) contribution to the CMB power spectrum at high  $\ell$ . The latest estimates using the CBI deep-field results [29,30] and ACBAR and Berkeley-Illinois-Maryland-Association Array [31] data suggests a value of  $\sigma_8^{\text{SZ}} = 0.98^{+0.12}_{-0.21}$  [32] with large errors due mainly to the non-Gaussian nature of the SZE. A joint analysis of pre-WMAP CMB, 2dF, and RCS data was carried out in Wang *et al.* [33] with similar results although CMB + weak lensing only results were not reported in that work and there was no marginalization over the source redshift distribution.

Our result for the Hubble parameter is consistent within  $1\sigma$  with the Hubble Space Telescope key-project result [34] but has smaller errors. Similarly, the value for the matter density  $\Omega_m = 0.30 \pm 0.03$  is consistent with other determinations, although our value for  $\Omega_m h^2$  is

TABLE I. Marginalized constraints for a selection of parameters. The left column uses only CMB data, the right column is for CMB and RCS data. The only external prior included for both results is a Gaussian BBN prior of  $0.022 \pm 0.002$ . All errors are 68% confidence intervals.

$(\Omega_{tot} = 1)$	BBN + CMB <sup>a</sup>	BBN + CMB <sup>a</sup> + RCS
$\Omega_b h^2$	$0.023 \pm 0.001$	$0.023 \pm 0.001$
$\Omega_c h^2$	$0.112 \pm 0.016$	$0.121 \pm 0.005$
$h$	$0.73 \pm 0.06$	$0.70 \pm 0.03$
$z_{re}$	$15 \pm 5$	$15 \pm 4$
$n_s$	$0.97 \pm 0.03$	$0.97 \pm 0.03$
$10^{10} A_s$	$24 \pm 4$	$25 \pm 3$
$\Omega_\Lambda$	$0.74 \pm 0.07$	$0.70 \pm 0.03$
$\Omega_m$	$0.26 \pm 0.07$	$0.30 \pm 0.03$
$T_0$ (Gyrs)	$13.6 \pm 0.3$	$13.6 \pm 0.2$
$\sigma_8$	$0.84 \pm 0.09$	$0.89 \pm 0.05$
$\sigma_8 e^{-\tau}$	$0.73 \pm 0.08$	$0.78 \pm 0.02$
$\sigma_8 \Omega_m^{0.5}$	$0.43 \pm 0.09$	$0.48 \pm 0.02$
$\Omega_m h$	$0.19 \pm 0.03$	$0.21 \pm 0.01$
$\Omega_m h^{2.3} (\sigma_8 e^{-\tau})^{-0.9}$	$0.163 \pm 0.003$	$0.162 \pm 0.002$

<sup>a</sup>WMAP( $\ell < 900$ ) + CBI, ACBAR, VSA( $\ell > 800$ ).

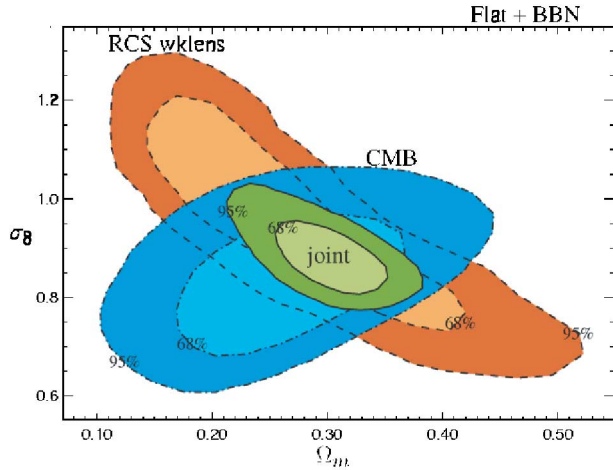


FIG. 2 (color online). The two-dimensional, marginalized likelihoods for the  $(\Omega_m, \sigma_8)$  plane. The overlaid, filled contours show the 68% and 95% integration levels for the distributions. Bottom: RCS only; middle: CMB only; top: CMB + RCS.

somewhat higher than that of [10]. We note however that CMB + 2dF only chains [22] give values for  $\Omega_m h^2$  very close to the CMB + RCS result reported in this work. The addition of RCS data leaves estimates of the scalar spectral tilt  $n_s$  essentially unaffected. This is due to the small range of scales probed by the RCS weak lensing results. Future surveys will most certainly have much more leverage on  $n_s$  as they will probe a range in scales an order of magnitude larger.

We have shown how CMB and weak lensing results can be combined to obtain constraints on cosmological parameters that depend on observations that have simple physical interpretations. Although only first generation weak lensing data are currently available, our approach yields results with errors comparable to or even smaller than those obtained using CMB in combination with other types of surveys. These results are encouraging for the use of next generation weak lensing surveys in deriving robust parameter fits. In particular the Canada–France–Hawaii–Telescope Legacy Survey  $\sim 170$  sq deg cosmic shear project will be a major step forward in the field of weak lensing.

The increasing accuracy in the determination of the source redshift distribution in future surveys will also help in reducing uncertainties and systematics tied to any intrinsic alignment in the ellipticity of nearby sources. It will also introduce the possibility of resolving separate redshift contributions to the convergence power spectrum [Eq. (1)] thus enhancing the parameter fitting ability of the observations.

We conclude that the combined CMB, weak lensing approach to parameter determination already constitutes a competitive alternative to other combinations and holds much promise for future investigations.

It is a pleasure to thank Dick Bond, Ue-Li Pen, and Dmitry Pogosyan for useful discussions. We acknowledge

the RCS team for use of their data. Research at CITA is supported by NSERC and the Canadian Institute for Advanced Research. The computational facilities at CITA are funded by the Canadian Fund for Innovation. C. R. C. acknowledges the Kavli Institute for Theoretical Physics (National Science Foundation Grant No. PHY99-07949) where part of this work was carried out.

\*Electronic address: [contaldi@cita.utoronto.ca](mailto:contaldi@cita.utoronto.ca)

<sup>†</sup>Department of Astronomy & Astrophysics, University of Toronto, 60 St. George Street, Toronto, M5S 3H8, ON, Canada

- [1] C. L. Bennett *et al.*, arXiv:astro-ph/0302207.
- [2] G. Hinshaw *et al.*, arXiv:astro-ph/0302217.
- [3] A. D. Miller *et al.*, *Astrophys. J.* **524**, L1, (1999).
- [4] J. E. Ruhl *et al.*, arXiv:astro-ph/0212229.
- [5] A. T. Lee *et al.*, *Astrophys. J.* **561**, L1, (2001).
- [6] N. W. Halverson *et al.*, *Astrophys. J.* **568**, 38 (2002).
- [7] T. J. Pearson *et al.*, arXiv:astro-ph/0205388.
- [8] K. Grainge *et al.*, arXiv:astro-ph/0212495.
- [9] C. I. Kuo *et al.*, arXiv:astro-ph/0212289.
- [10] D. N. Spergel *et al.*, arXiv:astro-ph/0302209.
- [11] L. Verde *et al.*, arXiv:astro-ph/0302218.
- [12] A. Kogut *et al.*, arXiv:astro-ph/0302213.
- [13] L. Page *et al.*, arXiv:astro-ph/0302220.
- [14] M. Colless *et al.*, *Mon. Not. R. Astron. Soc.* **328**, 1039, (2001).
- [15] R. A. C. Croft *et al.*, *Astrophys. J.* **581**, 20, (2002).
- [16] N. Kaiser, *Astrophys. J.* **284**, L9, (1984).
- [17] D. Bacon, A. Refregier, and R. Ellis, *Mon. Not. R. Astron. Soc.* **318**, 625, (2000).
- [18] H. Hoekstra, H. K. Yee, M. D. Gladders, L. F. Barrientos, P. B. Hall, and L. Infante, arXiv:astro-ph/0202285.
- [19] N. Kaiser, G. Wilson, and G. A. Luppino, arXiv:astro-ph/0003338.
- [20] L. van Waerbeke *et al.*, *Astron. Astrophys.* **358**, 30 (2000).
- [21] H. Hoekstra, H. Yee, and M. Gladders, *Astrophys. J.* **577**, 595 (2002).
- [22] <http://cosmologist.info/cosmomc/>
- [23] A. Lewis and S. Bridle, *Phys. Rev. D* **66**, 103511 (2002).
- [24] P. Schneider, L. van Waerbeke, B. Jain, and G. Kruse, *Mon. Not. R. Astron. Soc.* **296**, 873, (1998).
- [25] A. Lewis, A. Challinor, and A. Lasenby, *Astrophys. J.* **538**, 473 (2000).
- [26] R. E. Smith *et al.*, arXiv:astro-ph/0207664.
- [27] J. A. Peacock and S. J. Dodds, *Mon. Not. R. Astron. Soc.* **280**, L19, (1996).
- [28] D. Tytler, J. M. O'Meara, N. Suzuki, and D. Lubin, arXiv:astro-ph/0001318.
- [29] J. R. Bond *et al.*, arXiv:astro-ph/0205386.
- [30] B. S. Mason *et al.*, arXiv:astro-ph/0205384.
- [31] K. S. Dawson *et al.*, *Astrophys. J.* **581**, 86 (2002)
- [32] J. H. Goldstein *et al.*, arXiv:astro-ph/0212517.
- [33] X. Wang, M. Tegmark, B. Jain, and M. Zaldarriaga, arXiv:astro-ph/0212417.
- [34] W. L. Freedman *et al.*, *Astrophys. J.* **553**, 47 (2001).